

# MEASUREMENT OF LATERAL EARTH PRESSURES ON AN EMBEDDED FOUNDATION DURING EARTHQUAKES AND FORCED VIBRATION TESTS

CHIKAHIRO MINOWA

NIED 3-1 Tennoudai Tsukuba Ibaraki 305-0006 JAPAN, minowa@bosai.go.jp

ATSUMI SADOHIRA

Science University of Tokyo, 2641 Yamazaki, Noda, Chiba 278-8510 JAPAN j7100615@rs.noda.sut.ac.jp

## Abstract

The dynamic earth pressures during earthquakes and forced vibration tests have been observed on both sides of an embedded foundation. About 30 seismic events were observed. Some characteristics of dynamic earth pressures were extracted from the seismic observations. The main findings obtained in this study can be summarized as follows. (1) In the seismic events, the phase characteristics of earth pressures between both sides of the foundation show remarkable dependence on the frequency components of ground acceleration motions, and in phase for ground motions including lower frequencies and out of phase for ground motions with higher frequencies. (2) The earth pressures on lateral sides of the foundation are strongly related to horizontal velocity motions of the foundation. (3) The peak values of earth pressures show a tendency to increase with increase of lower frequencies contained in seismograms on the ground surface. (4) The fact that the earth pressure has strong relationship with the velocity motions of the foundation can be approximately explained by a simplified one-dimensional wave propagation theory for a soil rod model in earthquakes and force vibration tests.

**Key Words:** Earth Pressure, SSI, Earthquake Ground Motion, Forced Vibration Tests, Embedded Foundation.

## 1. Introduction

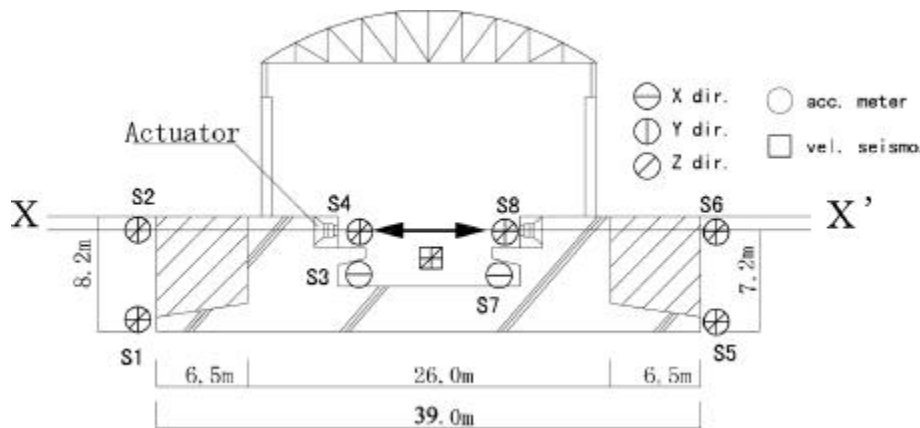
In seismic design of embedded foundations or underground structures, it becomes important to estimate earth pressures on foundations or underground walls during earthquakes. The observations of earth pressures during earthquakes, however, have been scarcely conducted [1, 2]. To make up for absence of the sufficient earthquake observations, there have been presented some experimental researches conducted in laboratories using small models [3, 4]. But most of them are limited inevitably to qualitative studies and do not seem to reproduce the actual earthquake motions.

The earth pressures during earthquakes would be affected by various factors such as frequency components of earthquake ground motions, the motions of foundations or underground structures, composition of soil layers and its properties around the structures, types of earthquake waves, incident angle of seismic waves and so on. It is preferable to examine the effect of each factor on the basis of earthquake observations. The recordings of dynamic earth pressures using a large scale shaking table foundation have been made on both sides of the foundation. In addition to the earth pressures, acceleration and velocity motions of the foundation as well as the free-field motions at the site have been also observed. The objective of this paper is to discuss the dynamic characteristics of lateral earth pressures on the rigid embedded foundation based on earthquake observations. Special emphases are placed in this study on the investigations about effects of the frequency components of earthquake ground motions and motions of the foundation on dynamic characteristics of the earth pressures.

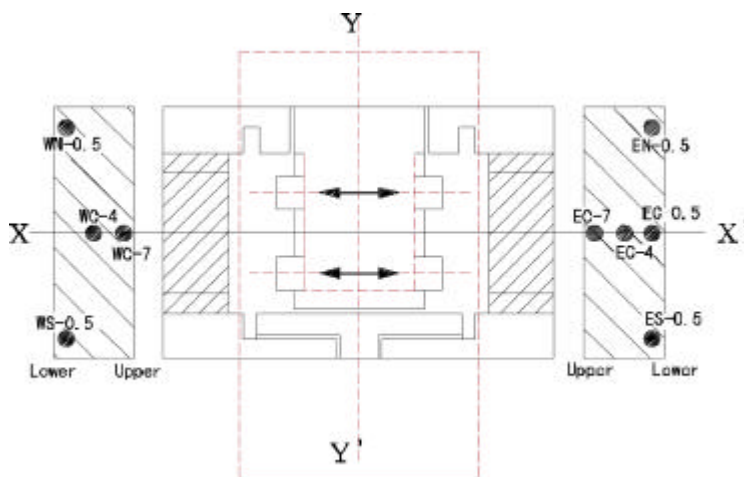
## 2. Outlines of Foundation and Earthquake Observation

### 2.1 OUTLINE OF FOUNDATION

The size of the foundation is 25m39m in plane and is used as a shaking table foundation in Tsukuba. The base of the foundation is directly supported on firm sand at a depth of 8.2m. The outlines of the foundation and soil profile are shown in figures 1(a), (b) and 2, respectively. The weight of the foundation itself and the shaking table is about 11,600 tf and 180 tf, respectively. The total weight corresponds almost to the excavated soil of the foundation. The fundamental frequency of the soil-foundation system is about 4.1 Hz in X direction.. It has been confirmed that the foundation behaves as a rigid body within frequencies less than 10 Hz. The detailed soil constants at the site were measured to a depth of about 40m and may be found elsewhere [5].



(a) Section of Foundation and Location of Seismographs



(b) Location of Earth Pressure Gauges.

Fig. 1 Outline of Foundation and Observation.

Shear wave velocity (m/s)	Density (tf/m <sup>3</sup> )	Poisson's Ratio	Depth (m)
82	1.3	0.497	G.L. -3m
145	1.6	0.492	-8m
230	1.7	0.492	-18m
400	1.7	0.474	-24m
480	1.9	0.462	-31m
320	1.7	0.484	-37m
400	1.9	0.474	40m

Fig. 2 Soil Profile

## 2.2 EARTHQUAKE OBSERVATION

Figure 1 (b) shows the location of earth pressure gauges on both sides of the foundation. On each side of the foundation, five earth pressure gauges (BE-2KR of Kyowa-Dengyo) have been instrumented at different depth of the embedded foundation, but one installed on the west side became out of function and is omitted from the figure. The observation of free-field ground motions has also been performed on the soil surface and at a depth of 40m. As for the foundation, the earthquake motions of the foundation have been observed at several points with seismographs and velocity seismographs as shown in figure 1(a). The motions of the foundation are represented by seismograms recorded at the point S3, which is located almost at the center of the foundation.

The records of dynamic earth pressures for about 30 earthquakes have been recorded for six years from 1991 to 1996. It includes incomplete records and they were omitted from analyses. The locations of epicenters of 20 earthquakes, which were used for the analyses are illustrated in figure 3 and the earthquake parameters are summarized in table 1. The observed peak accelerations in the EW direction on the free surface have been less than about 30 gals except the event of No. 22 as shown in table 1.

Table 1. Earthquake Parameters.

Eq.No	Date	Time	Hypocenter (N:N.L., E:E.L.)	Depth (km)	Mag. (M)	Max. of Acc (gal) (EW)	Group
1	1991. 6.25	12:48	N36.64, E140.97	49	5.1	31.96	C
2	8. 6	23:49	N35.87, E141.15	26	5.8	8.92	A
3	10.19	8:31	N36.08, E139.92	59	4.3	31.92	C
4	11.19	17:19	N35.60, E140.02	81	4.9	12.60	C
5	12.12	11:22	N36.46, E140.66	48	4.6	16.21	B
6	1992. 2. 2	4:04	N35.23, E139.79	92	5.9	18.71	B
9	5.11	19:04	N36.53, E140.54	56	5.6	29.28	B
10	6. 1	22:51	N36.67, E141.27	44	5.7	20.48	B
11	8.30	4:19	N33.20, E138.34	325	6.6	16.30	B
14	1993. 6. 7	16:47	N36.02, E141.76	28	5.9	9.32	B
16	9.18	11:18	N36.18, E140.88	35	5.0	16.21	B
17	10.12	0:55	N32.02, E138.24	390	7.0	24.96	B
21	1995. 1. 7	7:39	N40.18, E142.32	30	6.9	7.35	A
22	1. 7	21:34	N36.17, E139.59	70	5.4	100.47	B
23	1. 8	4:38	N36.19, E139.58	72	4.6	17.01	C
24	1.10	3:00	N35.56, E141.26	45	6.2	9.90	A
27	4.12	14:20	N36.27, E140.37	52	4.6	13.23	B
28	7. 3	8:53	N35.06, E139.30	120	5.6	5.80	B
29	7.30	3:11	N35.54, E140.36	50	5.0	20.90	B
30	1996. 9.11	11:37	N35.07, E141.03	30	6.6	26.52	A

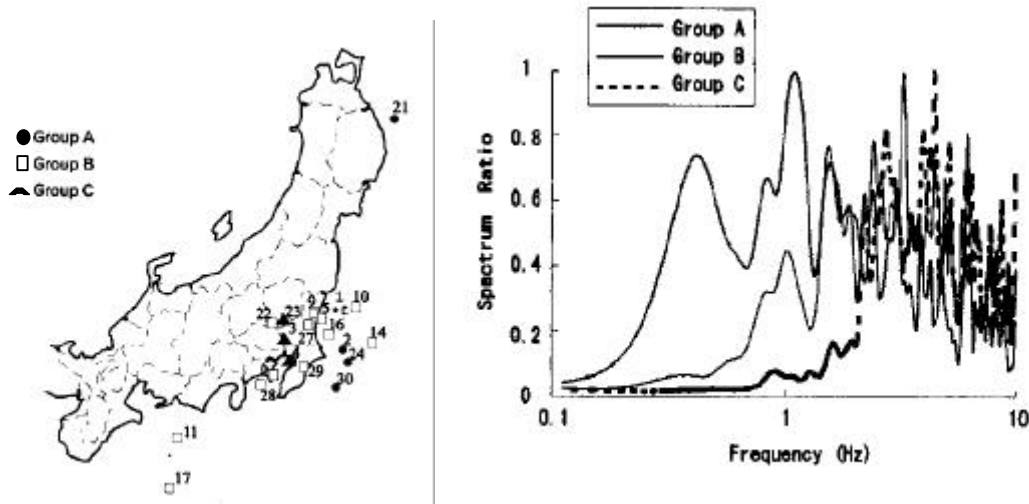


Fig.3 Location of Epicenters of Earthquakes. Fig.4 Fourier Spectra of Seismograms Chosen from Each Group

### 2.3 GROUPING OF EARTHQUAKE MOTIONS

In order to examine the effects of frequency components of earthquake ground motions on the earth pressures, all records were grouped into three (groups A, B and C) according to the frequency components of Seismograms recorded on the soil surface. Figure 4 shows Fourier spectra of the representative earthquake motions chosen from each group, which are shadily marked in table 1. The spectra shown in figure 4 are smoothed by the Parzen window and normalized by the maximum values. As seen from this figure, group A is characterized by the spectrum with predominant frequencies less than 1 Hz, and groups B and C, on the other hand, include less lower frequencies and more higher frequencies. In table 1 the categorized group symbols are listed for each earthquake.

### 3. Characteristics of Observed Earth Pressure in Earthquakes

#### 3.1 PHASE CHARACTERISTICS OF EARTH PRESSURES

Phase characteristics of earth pressures on both sides of the foundation can be extracted by calculating motion products of the earth pressures (product of two motions at every instance). The computed results are shown in figures 5(a), (b) and (c) for the representative motions of each group. The positive values of the motion product can be understood as the motions of earth pressures on both sides being in phase, and, on the contrary, the negative values imply that the two motions on both sides are out of phase 180 degrees. Inspection of the results shown in figure 5 (a) indicates that for the motions belonging to group A earth pressures on both sides are almost in phase throughout the record. It has been pointed out that the phenomenon of in phase motions of the earth pressures on two sides of a foundation cannot be explained by an analysis assuming the vertical incidence of seismic waves [2].

As for group B shown in figure 5(b), the earth pressures on both sides of foundation are showing opposite phase in primary portion of the motions and tend to shift into in phase with progress of time. With respect to motions of group C which contain higher frequencies, the out-of-phase and in phase of earth pressures appear alternately throughout the whole motions as shown in figure 5(c).

Summarizing the results shown in figure 5, it may be said that the phase characteristics of earth pressure between sides of the foundation are strongly affected by frequency components included in the ground motions and tend to be in phase for the motions with lower frequencies.

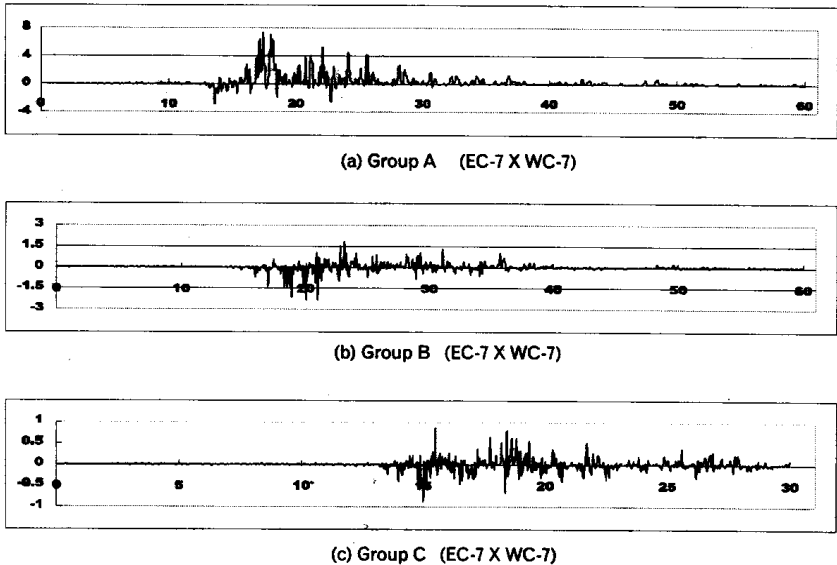


Fig. 5 Motion Products of Earth Pressures on Both Sides of Foundation

### 3.2 FOUNDATION MOTIONS AND EARTH PRESSURES

In order to study what motions of the foundation is related with the earth pressures, the displacement, velocity and acceleration motions of the foundation were compared, respectively, with the records of earth pressures. The displacement and velocity motions of the foundation were calculated by a numerical integration of acceleration motions observed at the point S3. It would be worth noting that thus computed velocity motions have shown almost the same as those recorded by a velocity seismometer on the foundation. Among the three kinds of motions, the strongest relation with earth pressures could be recognized for the velocity motions. In figures 6(a), (b) and (c), the velocity motions of the foundation are compared with those of earth pressures. The waveforms shown in figure 6 are normalized by corresponding maximum value.

In summarizing this section, it should be emphasized that the earth pressures on both sides of the foundation are strongly related with the horizontal velocity motions of the foundation.

### 3.3 MAXIMUM GROUND MOTIONS AND EARTH PRESSURES

It is important to estimate the peak values of earth pressures when subjected to earthquake excitations. Figures 7(a) and (b) show the relationship between the peak ground accelerations on the soil surface and maximum earth pressures at points WC-4 and EC-7. The results are plotted with different marks for each group. It will be noticed that the clear correlation between the peak seismograms and peak earth pressures can be obtained by grouping the earthquake ground motions as described above. The slope for each group was drawn by means of the least-squares method. It should be noted that the slopes clearly differ with different groups, and tend to increase in order of groups C, B and A. This fact suggests that the earth pressures tends to increase with increasing of lower frequencies contained in the ground motions. Taking an example for the earth pressures at point WC-4, the relationship between the maximum earth pressures Pomax (kPa) and the peak surface accelerations can be approximated by following equations;

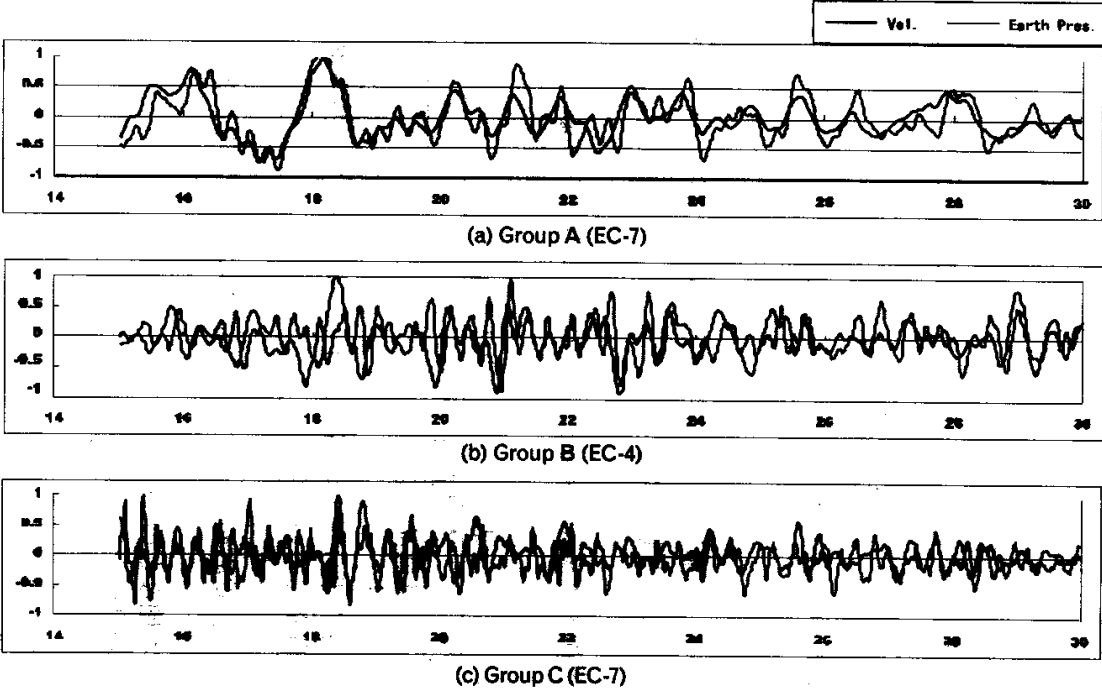


Fig.6. Comparison between Velocity Motions of Foundation and Earth Pressures.

$$\begin{aligned}
\text{Group A} \cdots \cdots p_{o \max} &= 0.22 \ddot{z}_{\max} \cdots \cdots (1-a) \\
\text{Group B} \cdots \cdots p_{o \max} &= 0.085 \ddot{z}_{\max} \cdots \cdots (1-b) \\
\text{Group B} \cdots \cdots p_{o \max} &= 0.046 \ddot{z}_{\max} \cdots \cdots (1-c) \\
\ddot{z} : \text{Acceleration} (cm/s^2)
\end{aligned}$$

Similarly, figure 8 indicates the relationship between the maximum ground velocities on the soil surface and the peak values of earth pressures at point WC-4. It will be noticed from the figure that the relationship between peak ground velocities and maximum values of earth pressures almost identical regardless of groups. This fact apparently indicates that the earth pressures are less frequency dependent on velocity ground motions. An approximate expression correlating the maximum earth pressures  $p_{o \max}$  (kPa) with the peak surface velocities for a point WC-4 can be written as,

$$\begin{aligned}
p_{o \max} &= 1.8 \dot{z} \cdots \cdots (2) \\
\dot{z} : \text{velocity} (cm/s)
\end{aligned}$$

The coefficients of above expressions might be subjected to modifications for different observation points and with change of the soil properties around foundation, and therefore it is suggested to be careful in applying the equations to other cases with different conditions. The presence of more general expressions for estimation of the maximum earth pressures is desired but left for future studies.

#### 4. Simplified Method to Predict Relationship between Velocity Motions of Foundation and Earth Pressures

##### 4.1 SIMPLIFIED SOIL MODEL

As stated in the section 3.2, the earth pressures on the lateral sides of the foundation are strongly related with the horizontal velocity motions of the foundation. We try in this section to explain the fact with a simplified method by a one-dimensional soil rod for the lateral soil which might be considered to resist to horizontal motions of the foundation. Figure 9(a) and (b) show a foundation-soil model and a soil rod extracted from the lateral soil surrounding the foundation. It is assumed here that the soil rod is extending

$$\frac{\partial^2 u}{\partial x^2} = \frac{\mathbf{r}}{E} \frac{\partial^2 u}{\partial t^2} \quad (3)$$

infinitely to the lateral direction and having a uniform section and homogeneous soil constants. It is also assumed that the rod is free from constraint along sides of the rod. The equation of motion with respect to an axial displacement of the rod,  $u(x,t)$  can be expressed by a well-known wave equation as follows; where  $x$  is the axial coordinate,  $\rho$  and  $E$  are mass density and Young modulus of the soil rod, respectively. Considering only the wave traveling in the positive direction of  $x$ -axis, the solution of equation (3) can be expressed as follows,

$$\begin{aligned}
u(x,t) &= f(x-ct) \quad (4) \\
\text{where} \quad c &= \sqrt{E/\mathbf{r}}
\end{aligned}$$

where  $f(\ )$  is an arbitrary function of the argument, which represents a longitudinal wave velocity of the soil rod. Supposing that the end of the rod is subjected to longitudinal excitation, we will have the following boundary condition at

$$E \frac{\partial u}{\partial x} \Big|_{x=0} = -p_o(t) \quad (5)$$

where  $p_o(t)$  is the normal excitation force per unit area. Applying the forward difference formulas in equation (5), we obtain an approximate expression for  $p_o(t)$  as shown below.

$$p_o = E \frac{u_o - u_1}{\Delta x} \quad (6)$$

where  $u_o$  corresponds to lateral displacement at the end of rod and  $u_1$  is displacement in the soil rod at a small distance from the end. Equation (6) suggests the validity of a method to estimate the earth pressure based on a relative displacement between the foundation and the soil. Equation (1) is one possibility to estimate the earth pressure. An alternative form to estimate the earth pressure can be obtained from equation (5), by making use of a relation  $du/dx = -\text{velocity}/c$  at  $x=0$ , and substitution from the relation into equation (5) leads to

$$p_o(t) = \frac{E}{c} v_o(t) \quad (7)$$

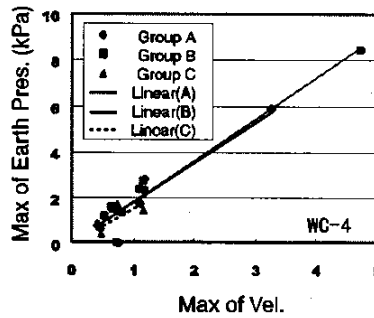
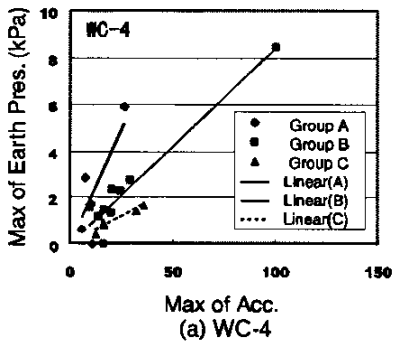


Fig 8. Peak Ground Velocities vs. Max of Earth Pressures (WC-4)

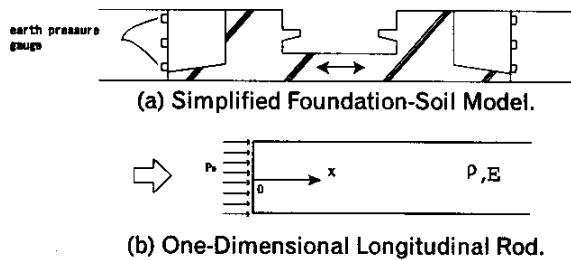
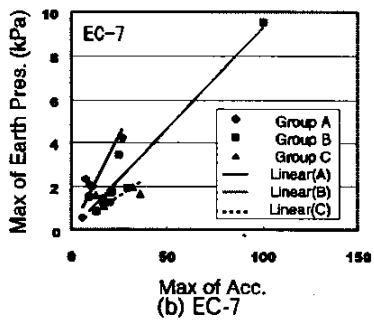


Fig 7. Peak Ground Acceleration vs. Max of Earth Pressure      Fig. 9 Resistance of Lateral Soil against Foundation Motions.

in which  $V_o$  corresponds to velocity motions at the end of the soil rod. The  $P_o(t)$  in equation (7) corresponds to the earth pressure acting on sides of the foundation, and therefore the equation indicates that the earth pressure is proportional to the velocity motions of the foundation.

## 4.2 NUMERICAL EXAMINATION OF EARTHQUAKES

In order to validate equation (7) numerically, we introduce soil constants for this equation. As for the value of a longitudinal wave velocity  $c$ , it might be appropriate to use the Lysmer's analog velocity, which has been used successfully to estimate soil reaction against piles. The Lysmer's analog velocity is defined as follows [6].

$$c = V_{La} = \frac{2.4}{\rho(1-\nu)} V \quad (8)$$

where  $\nu$  and  $V_s$  are the Poisson ratio and shear wave velocity of a soil. Furthermore, the corresponding Young modulus may be evaluated by

$$E_a = \rho V_{La}^2 \quad (9)$$

The value  $E_a$  is to be used for the Young modulus of the soil rod  $E$ . Thus, the ratio between the peak values of velocity motions of the foundation and earth pressures ( $P_{0max}/V_{0max}$ ) may be expressed using new symbols as follows;

$$\frac{P_{0max}}{V_{0max}} = \frac{E_a}{V_{La}} \quad (10)$$

Table 2. Surface Soil Constants and  $E_a/V_{La}$  vs.  $P_{0max}/V_{0max}$

Surface Soils	Soil const.				$E_a/V_{La}$	Measured Soil pres. ( $P_{0max}/V_{0max}$ )		
	$V_s$	$\nu$	$\gamma$	Thickness		Group A	Group B	Group C
①	82	0.497	1.3	3.0	23.4	5~21	10~38	19~52
②	145	0.492	1.6	5.2	50.4			
	m/s		tf/m <sup>3</sup>	m	gf/m <sup>2</sup> / m/s	gf/m <sup>2</sup> / m/s		

In equation (10), it is assumed that the peak values of the earth pressure and the velocity motion of the foundation occur simultaneously. The observed peak ratios shown in the left side of above equation were compared with the results of  $E_a/V_{La}$  evaluated by use of the measured soil constants. The lateral soil of the foundation is composed of two layers and the shear wave velocities ( $V_s$ ), the Poisson's ratios ( $\nu$ ) and soil densities ( $\gamma$ ) have been obtained as shown in table 2. This table also shows the comparison between the computed values of  $E_a/V_{La}$  for each layer and the ratios of observed peak values  $P_{0max}/V_{0max}$  for each group. Inspection of the results shown in table 2 reveals that the ratios of  $P_{0max}/V_{0max}$  tend to increase in order of group A, B and C. The fact is indicating that the ratios are frequency dependent. It will be also noticed that though the ratios of observed peak values differ depending on the group and with varying observation points the computed results of  $E_a/V_{La}$  based on the actual soil constants correspond almost to the ratios of observed peak values  $P_{0max}/V_{0max}$ . This fact perhaps suggests that a part of dynamic characteristics of the earth pressures on the foundation may be explained roughly by use of a simplified model considered above. Inspecting the results shown in table 2, it will be noticed that the measured results of  $P_{0max}/V_{0max}$  tends to increase in order of group C, B and A, and thus the earth pressures for the velocity motions of the foundation seem to be frequency dependent. The frequency characteristics of the earth pressure, however, can be explained by the simplified model considered here and more sophisticated model must be introduced to explain the phenomena.



## 5 Forced Vibration Tests and Numerical Examinations

### 5.1 FORCED VIBRATION TESTS

On the foundation, the shaking table is installed. The table is driven by hydraulic powers in the lateral direction. Four hydraulic actuators are set up between the table and the foundation, shown as figures. 1. The foundation was excited in sinusoidal waves of 1Hz – 20Hz with the force of 18tf, approximately. The drive force for the table, the responses of the foundation and the earth pressures of both sides in the foundation were measured.

### 5.2 NUMERICAL EXAMINATIONS OF FORCED VIBRATION TESTS

The scheme of modeling is explained in figure 10. Two soil layers on the side walls of foundation were considered in the analysis. The simplified lumped mass model shown in figure 11 was used for two layers of the lateral soil. The left end of the model was excited.

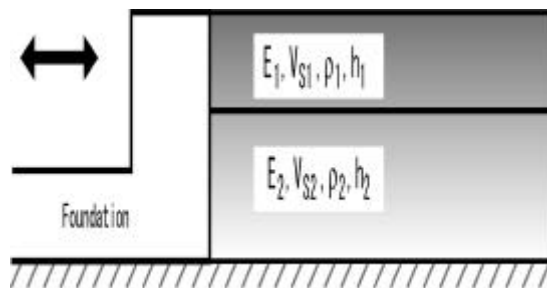


Fig.10 Schematic Model of Forced Vibration.

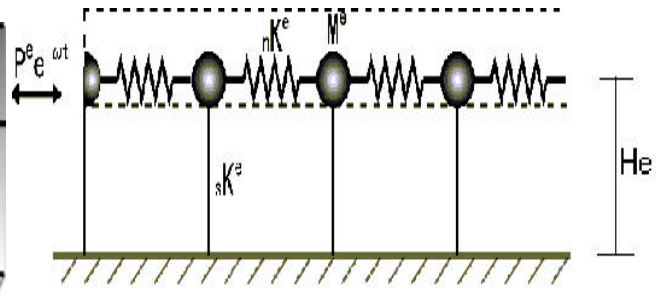


Fig.11 Simplified Analysis Model

The figure 12, 13, 14 are the comparisons between tests and numerical evaluation results. Fig.12 is the phase characteristics. Fig. 13 is the frequency characteristics of earth pressure versus velocity amplitudes. Fig. 14 is the frequency characteristics of earth pressure versus displacement amplitudes. In the forced vibration tests, the earth pressures shows constant to displacements in the frequencies less than 4Hz, and to velocities in the frequencies more than 4Hz that the fundamental frequency of the lateral soil.

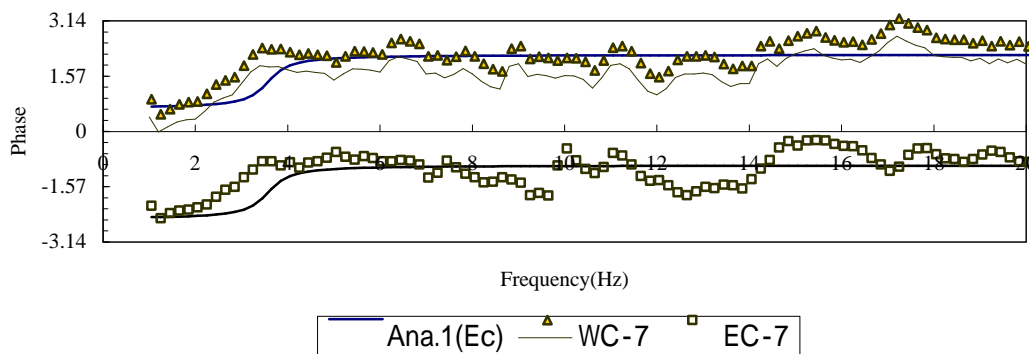


Fig. 12 Phase Characteristic Between earth Pressures and Foundation Velocities

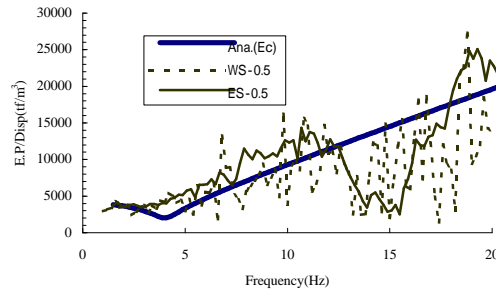
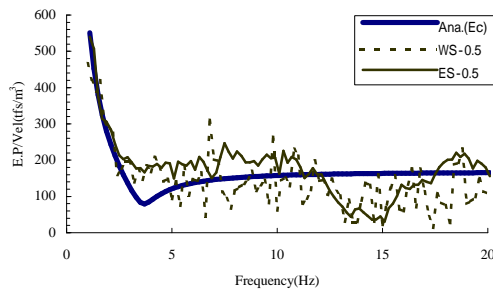


Fig. 12 Frequency Characteristics of Earth Pressure Versus Foundation Velocities.

Fig. 13 Frequency Characteristics of Earth Pressure Versus Foundation Displacements

## 6. Conclusions

In this paper, characteristics of dynamic earth pressures during earthquakes were examined on the basis of observations for about 20 events recorded on the lateral sides of an embedded foundation. It was found that the earth pressures on both side of the foundation tend to be in phase for earthquake ground motions including relatively lower frequencies. On the contrary, for ground motions with higher frequencies the earth pressures on both sides tend to be out of phase. These facts are clearly indicating that the phase characteristics of lateral earth pressures on both sides of the foundation are influenced greatly by frequency components of earthquake motions. In addition, it was revealed that the lateral earth pressures were strongly related to the horizontal velocity motions of the foundation. It was also shown that a part of these characteristics could be approximately explained by using a simplified one-dimensional soil model. In the forced vibration tests, the simplified lumped mass model could explain the test results very well.

## 7. Acknowledgment

The authors would like to express their gratitude to Ms. Aya Shigetoh and Mr. Takayoshi Mutoh for their help in preparation of this paper.

The analysis was conducted as a cooperative study between NIED and Iguchi Laboratory in Science University of Tokyo.

## References

1. Onimaru, S., Sugawara, R., Uetake, T., Sugimoto, M. and Ohmiya, Y. (1994) Dynamic characteristics of earth pressure on seismic array observation (in Japanese), Proc. 9th Japan Earthq. Engng. Symp., pp1051-1056.
2. Uchiyama, S. and Yamashita, T. (1999) Experimental and analytical studies of lateral seismic earth pressure on a deeply embedded building model (in Japanese), J. of Struct. and Constr. Engng., Trans. of AIJ, No. 516, pp105-112.
3. Kazama, M. and Inatomi, T. (1988) A study on seismic stability of large scale embedded rigid structures, Proc. 9th WCEE (Tokyo-Kyoto), Vol. III, III-629-III-634.
4. Watanabe, K., Maeda, T., Kobayashi, Y. and Towhata, I. (1998) Shaking table tests on seismic earth pressure exerted on retaining wall model, Proc. the 3rd Symp. on Urban Earthq. Hazard to Near-Field Earthquakes, National Science Fund of Ministry of Education of Japan, pp219-222.
5. Minowa, C., Ohyagi, N., Ogawa, N., and Ohtani, K. (1991) Response data of large shaking table foundation during improvement works (in Japanese), Tech. Note of the National Research Institute for Earth Science and Disaster Prevention, No.151.
6. Gazetas, G. and Dobry, R. (1984) Horizontal response of piles in layered soils, J. Geotech. Engng, ASCE, Vol. 110, No. 1, pp20-40.